Compressed Sensing Based Channel Estimation and Impulsive Noise Cancelation in Underwater Acoustic OFDM Systems

Peng Chen*, Yue Rong*, Sven Nordholm*, Alec J. Duncan†

*Department of Electrical and Computer Engineering
†Department of Imaging and Applied Physics
Curtin University, Bentley, WA 6102, Australia

Zhiqiang He
Key Laboratory of Universal Wireless Communication
Beijing University of Posts and Telecommunications
Beijing 100876, China

Abstract—**Impulsive noise occurs frequently in underwater acoustic (UA) channels and can significantly degrade the performance of UA orthogonal frequency-division multiplexing (OFDM) systems. In this paper, we propose a novel compressed sensing based algorithm for joint channel estimation and impulsive noise cancelation in UA OFDM systems. The proposed algorithm jointly estimates the channel impulse response and the impulsive noise by utilizing the pilot subcarriers. The estimated impulsive noise is then converted to the time domain and removed from the received signals. The proposed algorithm is applied to process the data collected during the UA communication experiment conducted in December 2015 in the estuary of the Swan River, Western Australia. The results show that the proposed approach improves the performance of both channel estimation and impulsive noise mitigation.**

I. INTRODUCTION

The underwater acoustic (UA) channel, especially shallow water UA channel, is one of the most challenging channels for wireless communication, due to its extremely limited bandwidth, severe fading, strong multipath interference, and significant Doppler shifts [1]. In the past decades, significant advances have been made in high data rate UA communications [1], [2]. Among them, UA orthogonal frequency-division multiplexing (OFDM) systems have attracted much research interest, due to their strong capability in mitigating inter-symbol interference (ISI) with a large delay spread [3], [4].

In addition to the above challenges, UA communication is also impacted by impulsive noise which is introduced by natural sources and human activities [5]. It is reported in [5] that impulsive noise can significantly degrade the performance of UA OFDM systems. Recently, impulsive noise mitigation for OFDM systems received increasing attention in UA communications [5], [6].

In this paper, we propose a novel compressed sensing (CS) based algorithm for joint channel estimation and impulsive noise cancelation in UA OFDM systems by exploiting the sparsity of both the UA channel and the impulsive noise. Once the impulsive noise is estimated using the pilot subcarriers, it is transformed to the time domain using a least-squares (LS) based method and removed from the received signals before channel equalization. We show that the proposed algorithm
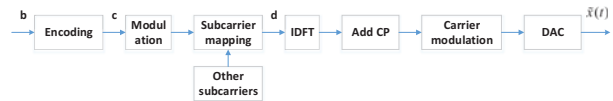

Fig. 1. Block diagram of the transmitter in a UA OFDM system.

successfully improves the accuracy of channel estimation, as the existence of impulsive noise is explicitly considered during channel estimation.

The proposed algorithm is applied to process the data collected during the UA communication experiment conducted in December 2015 in the estuary of the Swan River, Western Australia. The results show that the proposed approach is able to mitigate the impulsive noise in UA OFDM communication systems and improve the system bit-error-rate performance.

II. SYSTEM MODEL

In this paper, we consider a frame based coded UA OFDM system. As shown in Fig. 1, at the transmitter end, in each frame, a binary source data stream $\boldsymbol{b} = (b[1], \ldots, b[L_b])^T$ is encoded, interleaved, and punctured to form a coded sequence $\boldsymbol{c} = (c[1], \ldots, c[L_c])^T$ with length $L_c = R_m N_s N_b$, where $(\cdot)^T$ denotes the matrix (vector) transpose, L_b is the number of source bits in each frame, R_m denotes the modulation order, N_s is the number of data subcarriers, and N_b denotes the number of OFDM blocks in one frame. The coded sequence $\boldsymbol{c}$ is mapped into $N_s N_b$ data symbols taken from the quadrature phase-shift keying (QPSK) constellations. Then every N_s data symbols together with N_p QPSK modulated pilot symbols are mapped into one OFDM symbol vector $\boldsymbol{d} = (d[1], \ldots, d[N_c])^T$, where N_p and $N_c \geq N_p + N_s$ are the number of pilot subcarriers and total subcarriers, respectively. We denote $\mathcal{I}_p$ as the indices of pilot subcarriers. We assume that pilot subcarriers are uniformly spaced and denote $\boldsymbol{d}_p$ as the pilot sequence in one OFDM block.

Passband signals are directly generated for each OFDM block at the transmitter. Let f_{sc} denote the subcarrier spacing. The bandwidth of the transmitted signal is $B = f_{sc}N_c$ and the duration of one OFDM symbol is $T = 1/f_{sc}$. The N_c

subcarriers are located at frequencies $f_k = f_c + kf_{sc}$, $k = -\frac{N_c}{2}+1, \ldots, \frac{N_c}{2}$, where f_c is the center carrier frequency. To enable simple one-tap equalization and to avoid interference among OFDM blocks, a cyclic prefix (CP) of length T_{cp} is prepended to the OFDM symbol, and the total length of one OFDM block is $T_{total} = T + T_{cp}$. The continuous time representation of an OFDM block can be expressed as

$$\tilde{x}(t) = 2\mathrm{Re}\left\{ \left[\frac{1}{\sqrt{N_c}} \sum_{k=-\frac{N_c}{2}+1}^{\frac{N_c}{2}} \check{d}[k] e^{j2\pi k f_{sc}t} \right] e^{j2\pi f_c t} \right\},$$
$$0 \le t \le T$$
$$\tilde{x}(t) = \tilde{x}(t+T), \qquad -T_{cp} \le t < 0 \qquad (1)$$

where $\mathrm{Re}\{\cdot\}$ denotes the real part of a complex number and

$$\check{d}[k] = \begin{cases} d[k], & 1 \le k \le \frac{N_c}{2} \\ d[k+N_c], & -\frac{N_c}{2}+1 \le k \le 0 \end{cases}.$$

A general UA channel with L_p paths can be represented as

$$h(t, \tau) = \sum_{l=1}^{L_p} A_l(t)\delta(t - \tau_l(t)) \qquad (2)$$

where $A_l(t)$ and $\tau_l(t)$ are the amplitude and delay of the lth path, respectively, and we assume $T_{cp} > \tau_{L_p}(t)$. In general, UA communication suffers from time-varying frequency offset caused by the change of $\tau_l(t)$ within one OFDM block. As this paper focuses on joint channel estimation and impulsive noise cancelation, we consider that the frequency offset is properly removed at the receiver. Thus, in the following, we assume that $A_l(t)$ and $\tau_l(t)$ are constant during one OFDM block. Then the received passband signal of one OFDM block is given by

$$\tilde{r}(t) = 2\mathrm{Re}\left\{ \sum_{l=1}^{L_p} A_l \tilde{x}(t - \tau_l) \right\} + \tilde{v}(t) + \tilde{w}(t) \qquad (3)$$

where $\tilde{v}(t)$ is the passband impulsive noise and $\tilde{w}(t)$ represents other non-impulsive background noise. After removing the CP, downshifting, and low-pass filtering $\tilde{r}(t)$, the baseband received signal can be obtained from (1) and (3) as

$$r(t) = \sum_{l=1}^{L_p} \frac{A_l e^{-j2\pi f_c \tau_l}}{\sqrt{N_c}} \sum_{k=-\frac{N_c}{2}+1}^{\frac{N_c}{2}} \check{d}[k] e^{j2\pi k f_{sc}(t-\tau_l)} + v(t) + w(t)$$
$$= \frac{1}{\sqrt{N_c}} \sum_{k=-\frac{N_c}{2}+1}^{\frac{N_c}{2}} \check{d}[k] e^{j2\pi k f_{sc}t} \sum_{l=1}^{L_p} A_l e^{-j2\pi f_k \tau_l}$$
$$+ v(t) + w(t), \qquad 0 \le t \le T \qquad (4)$$

where $v(t)$ and $n(t)$ are the baseband impulsive noise and other noise, respectively. From (4), the channel frequency response at the kth subcarrier is given by

$$H[k] = \sum_{l=1}^{L_p} A_l e^{-j2\pi f_k \tau_l}, \quad k = -\frac{N_c}{2}+1, \ldots, \frac{N_c}{2}.$$

By sampling $r(t)$ at the rate of $1/B$, we obtain discrete time samples of one OFDM symbol from (4) as

$$r[i] = \frac{1}{\sqrt{N_c}} \sum_{k=-\frac{N_c}{2}+1}^{\frac{N_c}{2}} \check{d}[k] e^{j2\pi ik/N_c} H[k] + v[i] + w[i] \qquad (5)$$

for $i = 1, \ldots, N_c$, where $v[i]$ and $w[i]$ are the impulsive noise and other noise samples, respectively. The matrix-vector form of (5) is given by

$$\boldsymbol{r} = \boldsymbol{F}^H \boldsymbol{D} \boldsymbol{h}_f + \boldsymbol{v} + \boldsymbol{w} = \boldsymbol{F}^H \boldsymbol{D} \boldsymbol{F} \boldsymbol{h}_t + \boldsymbol{v} + \boldsymbol{w} \qquad (6)$$

where $(\cdot)^H$ denotes the conjugate transpose, $\boldsymbol{D} = \mathrm{diag}(\boldsymbol{d})$ is a diagonal matrix taking $\boldsymbol{d}$ as the main diagonal elements, $\boldsymbol{r} = (r[1], \ldots, r[N_c])^T$, $\boldsymbol{v} = (v[1], \ldots, v[N_c])^T$, $\boldsymbol{w} = (w[1], \ldots, w[N_c])^T$, $\boldsymbol{F}$ is an $N_c \times N_c$ discrete Fourier transform (DFT) matrix with the (i,k)-th entry of $1/\sqrt{N_c}e^{-j2\pi(i-1)(k-1)/N_c}$, $i, k = 1, \ldots, N_c$. In (6), $\boldsymbol{h}_f = (h_f[1], \ldots, h_f[N_c])^T$ is a vector containing the channel frequency response at all N_c subcarriers with

$$h_f[k] = \begin{cases} H[k], & 1 \le k \le \frac{N_c}{2} \\ H[k - N_c], & \frac{N_c}{2}+1 \le k \le N_c \end{cases}$$

and $\boldsymbol{h}_t = \boldsymbol{F}^H \boldsymbol{h}_f$ is the discrete time domain representation of the channel impulse response with a maximum delay of $L_m = \lceil B\tau_{L_p} \rceil$.

From (6), the frequency domain representation of the received signal can be written as

$$\boldsymbol{r}_f = \boldsymbol{F}\boldsymbol{r} = \boldsymbol{D}\boldsymbol{h}_f + \boldsymbol{v}_f + \boldsymbol{w}_f \qquad (7)$$

where $\boldsymbol{v}_f = \boldsymbol{F}\boldsymbol{v}$ and $\boldsymbol{w}_f = \boldsymbol{F}\boldsymbol{w}$ are the impulsive noise and other noise in the frequency domain, respectively.

III. PROPOSED APPROACH

The block diagram of various receivers is shown in Fig. 2, where CE denotes channel estimation and JCINE stands for the proposed joint channel and impulsive noise estimation algorithm. The proposed receivers correspond to branches labeled with (c) and (d) in Fig. 2.

Let us introduce an $N_p \times N_c$ matrix $\boldsymbol{P}$ which selects N_p pilot subcarriers out of total N_c subcarriers. Thus, $\boldsymbol{P}$ has unit entry at the $(i, \mathcal{I}_p[i])$-th position, $i = 1, \cdots, N_p$, and zero elsewhere. From (7), the received signals in the pilot subcarriers can be written as

$$\boldsymbol{r}_p = \boldsymbol{P}\boldsymbol{D}\boldsymbol{h}_f + \boldsymbol{P}\boldsymbol{v}_f + \boldsymbol{P}\boldsymbol{w}_f$$
$$= \boldsymbol{D}_p \boldsymbol{h}_p + \boldsymbol{v}_p + \boldsymbol{w}_p$$
$$= \boldsymbol{D}_p \boldsymbol{F}_p \boldsymbol{h}_{p,t} + \boldsymbol{F}_p \boldsymbol{v}_{p,t} + \boldsymbol{w}_p$$
$$= \boldsymbol{M}_p \boldsymbol{\alpha}_p + \boldsymbol{w}_p \qquad (8)$$

where $\boldsymbol{D}_p = \mathrm{diag}(\boldsymbol{d}_p)$, $\boldsymbol{h}_p$ contains the channel frequency responses at N_p pilot subcarriers, $\boldsymbol{F}_p$ is an $N_p \times N_p$ DFT matrix with the (i,k)-th entry of $1/\sqrt{N_p}e^{-j2\pi(i-1)(k-1)/N_p}$, $i, k = 1, \ldots, N_p$, and

$$\boldsymbol{v}_p = \boldsymbol{P}\boldsymbol{v}_f, \quad \boldsymbol{w}_p = \boldsymbol{P}\boldsymbol{w}_f, \quad \boldsymbol{h}_{p,t} = \boldsymbol{F}_p^H \boldsymbol{h}_p, \quad \boldsymbol{v}_{p,t} = \boldsymbol{F}_p^H \boldsymbol{v}_p$$
$$\boldsymbol{\alpha}_p = (\boldsymbol{h}_{p,t}^T, \ \boldsymbol{v}_{p,t}^T)^T, \quad \boldsymbol{M}_p = (\boldsymbol{D}_p \boldsymbol{F}_p, \ \boldsymbol{F}_p). \qquad (9)$$

Fig. 2. Block diagram of various receivers.

Fig. 3. Transmitter and receiver locations of the experiment.
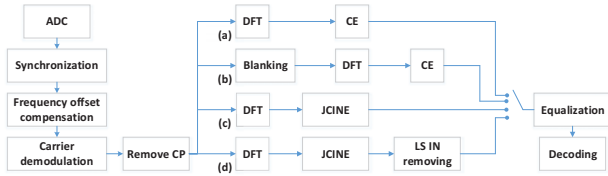
Fig. 4. Frame structure of the transmitted signals.

We select $N_p \geq L_m$, which means that all the non-zero entries of $\boldsymbol{h}_t$ are within its first N_p entries. In this case, $\boldsymbol{h}_t$ can be easily recovered from $\boldsymbol{h}_{p,t}$. Since the UA channel is sparse, only a few entries of $\boldsymbol{h}_{p,t}$ are non-zero. Moreover, $\boldsymbol{v}_{p,t}$ can be viewed as a 'fold-and-add' version of $\boldsymbol{v}$ which is considered to be sparse as well. Therefore, it is reasonable to assume that $\boldsymbol{\alpha}_p$ is sparse. As the dimension of $\boldsymbol{M}_p$ is $N_p \times 2N_p$, it is hard to recover $\boldsymbol{\alpha}_p$ from $\boldsymbol{r}_p$ using conventional linear estimators. However, by exploiting the sparsity of $\boldsymbol{\alpha}_p$, we can apply CS techniques to obtain an accurate estimation of $\boldsymbol{\alpha}_p$. In this paper, the orthogonal matching pursuit (OMP) algorithm [7] is applied to estimate $\boldsymbol{\alpha}_p$ in (8).

We would like to mention that as the existence of impulsive noise is explicitly considered by (8) during channel estimation, the proposed joint channel and impulsive noise estimation algorithm improves the accuracy of channel estimation. Let $\hat{\boldsymbol{\alpha}}_p = (\hat{\boldsymbol{h}}_{p,t}^T, \ \hat{\boldsymbol{v}}_{p,t}^T)^T$ denote the estimated $\boldsymbol{\alpha}_p$. From (8), the estimated channel frequency response in the pilot subcarriers can be obtained by

$$\hat{\boldsymbol{h}}_p = \boldsymbol{F}_p \hat{\boldsymbol{h}}_{p,t}. \tag{10}$$

One can use the improved channel estimation result in (10) to perform channel equalization as indicated by the branch marked with (c) in Fig. 2. The performance of this approach will be studied in Section IV.

The non-zero entries of $\boldsymbol{h}_t$ are all located within its first N_p entries, whereas the non-zero entries of $\boldsymbol{v}$ can appear at any of the N_c entries. Since $\boldsymbol{v}_{p,t}$ is a 'fold-and-add' version of $\boldsymbol{v}$, to obtain an estimation of $\boldsymbol{v}$ from $\boldsymbol{v}_{p,t}$, the positions of the impulsive noise need to be known in general. This can be done by a thresholding test, where the receiver firstly calculates the average power G of the current OFDM block and then collects the positions of possible impulsive noise into a vector $\mathcal{I}_I$ which satisfies

$$|r[\mathcal{I}_I[i]]|^2 > G\beta, \quad i = 1, \ldots, N_I. \tag{11}$$

Here β is a threshold parameter and N_I is the number of possible positions of impulsive noise.

Let us introduce $\boldsymbol{v}_I$ as a vector which contains all the N_I samples of impulsive noise in one OFDM block. Then the impact of $\boldsymbol{v}_I$ on the pilot subcarriers can be written as

$$\boldsymbol{v}_p = \boldsymbol{P}\boldsymbol{F}\boldsymbol{P}_I \boldsymbol{v}_I \tag{12}$$

where $\boldsymbol{P}_I$ is an $N_c \times N_I$ matrix indicating the position of the impulsive noise given by

$$\boldsymbol{P}_I[i,k] = \begin{cases} 1, & i = \mathcal{I}_I[k], k = 1, \ldots, N_I \\ 0, & \text{otherwise} \end{cases}.$$
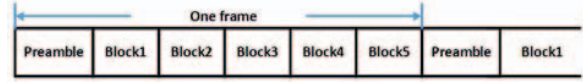
Note that an estimation of $\boldsymbol{v}_p$ can be obtained from (8) as

$$\hat{\boldsymbol{v}}_p = \boldsymbol{F}_p \hat{\boldsymbol{v}}_{p,t}. \tag{13}$$

Thus, using (12) and (13), $\boldsymbol{v}_I$ can be estimated as

$$\hat{\boldsymbol{v}}_I = (\boldsymbol{F}_I^H \boldsymbol{F}_I)^{-1} \boldsymbol{F}_I^H \hat{\boldsymbol{v}}_p = (\boldsymbol{F}_I^H \boldsymbol{F}_I)^{-1} \boldsymbol{F}_I^H \boldsymbol{F}_p \hat{\boldsymbol{v}}_{p,t} \tag{14}$$

where $\boldsymbol{F}_I = \boldsymbol{P}\boldsymbol{F}\boldsymbol{P}_I$ and $(\cdot)^{-1}$ stands for the matrix inversion. Then $\boldsymbol{v}$ is estimated by $\hat{\boldsymbol{v}} = \boldsymbol{P}_I \hat{\boldsymbol{v}}_I$. Finally, $\hat{\boldsymbol{v}}$ is subtracted from the received signal $\boldsymbol{r}$ as in branch (d) in Fig. 2 and the resulting signals are passed to channel equalization and decoding operations.

IV. EXPERIMENT RESULTS AND DISCUSSIONS

We apply the proposed algorithm to process the data recorded during a UA communication experiment conducted in December 2015 in the estuary of the Swan River, Western Australia. The locations of the transmitter and receiver are shown in Fig. 3, where the distance between the transmitter and receiver was 936 meters. The water depth along the direct path varied between 2.5 and 6 meters. Both the transmitter transducer and the receiver hydrophone were attached through cables to steel frames a half meter above the river bed. As the hydrophone was located in warm shallow water close to a jetty, there was a significant amount of highly impulsive snapping shrimp noise. Another source of impulsive noise during the experiment was from waves breaking at the jetty piers whose intensity increases with the wind speed. To investigate the impact of wind on the breaking wave noise, the same data file was transmitted three times during the day at different wind conditions. The data files recorded during these three transmissions were named T83, T84, and T85, respectively. Among these three files, the T84 file contains signals most heavily affected by the impulsive noise, while signals in the T83 file are least impacted by the impulsive noise.

Key parameters of the experimental system are summarized in Table I. Fig. 4 shows the frame structure of the transmitted signals. It can be seen that each frame contains $N_b = 5$ OFDM data blocks and one preamble block. The preamble block has the same length as a data block and is used for

Bandwidth	B	4 kHz
Carrier frequency	f_c	12 kHz
Number of subcarriers	N_c	512
Subcarrier spacing	f_{sc}	7.8 Hz
Length of OFDM symbol	T	128 ms
Length of CP	T_{cp}	25 ms

TABLE II
PERFORMANCE COMPARISON OF VARIOUS ALGORITHMS (T83 FILE).

Coding rate	Method	Raw BER	Coded BER	FER
1/3	LS w/o blanking	6.2%	0.2%	0.4%
	LS + blanking	5.2%	0	0
	JCINE w/o INC	5.0%	0	0
	JCINE LS INC	3.5%	0	0
1/2	LS w/o blanking	5.6%	0.3%	1.6%
	LS + blanking	4.7%	0	0
	JCINE w/o INC	4.6%	0	0
	JCINE LS INC	3.3%	0	0

TABLE III
PERFORMANCE COMPARISON OF VARIOUS ALGORITHMS (T84 FILE).

Coding rate	Method	Raw BER	Coded BER	FER
1/3	LS w/o blanking	18.7%	10.9%	50.4%
	LS + blanking	15.5%	1.3%	7.3%
	JCINE w/o INC	16.7%	6.5%	30.5%
	JCINE LS INC	14.7%	0.5%	4.1%
1/2	LS w/o blanking	18.1%	22.5%	93.6%
	LS + blanking	14.6%	15.9%	84.7%
	JCINE w/o INC	16.0%	19.3%	87.9%
	JCINE LS INC	13.5%	10.9%	61.7%

TABLE IV
PERFORMANCE COMPARISON OF VARIOUS ALGORITHMS (T85 FILE).

Coding rate	Method	Raw BER	Coded BER	FER
1/3	LS w/o blanking	13.5%	1.6%	6.4%
	LS + blanking	11.2%	0	0
	JCINE w/o INC	11.6%	0.7%	2.4%
	JCINE LS INC	9.1%	0	0
1/2	LS w/o blanking	15.0%	15.3%	71.6%
	LS + blanking	11.7%	3.9%	24.8%
	JCINE w/o INC	12.8%	9.5%	50.8%
	JCINE LS INC	9.8%	0.5%	5.2%

synchronization. Among the 512 subcarriers, there are 325 data subcarriers and 128 uniformly spaced pilot subcarriers. The data symbols are modulated by QPSK constellations encoded by 1/2 or 1/3 rate turbo codes. The number of source bits in each frame is $L_b = 1632$ (1/2 rate) or $L_b = 1088$ (1/3 rate). Thus, the system source data rate is

$$R_b = \frac{L_b}{(T+T_{cp})(N_b+1)} = \begin{cases} 1.19 \text{ kb/s}, & 1/3 \text{ rate} \\ 1.78 \text{ kb/s}, & 1/2 \text{ rate} \end{cases}.$$

Each transmission contains 500 frames with 250 frames for every coding rate.

The bit-error-rate (BER) and the frame-error-rate (FER) performances of the following algorithms (branches (a)-(d) in Fig. 2) are shown in Tables II-IV for three recorded files.

(a) LS channel estimator without the blanking operation.
(b) LS channel estimator after blanking of the impulsive samples detected at the positions of $\mathcal{I}_I$ (11).
(c) Proposed algorithm without impulsive noise cancelation (INC).
(d) Proposed algorithm with LS based INC.

It can be seen from Tables II-IV that compared with the LS estimator without the blanking operation, the proposed algorithm without INC can reduce the raw (uncoded) BER by around 1% for the T83 file and 2% for the T84 and T85 files, and the coded BER by 3-4% for the T84 file and 6% for the T85 file with 1/2 rate. Such gain is contributed by an improved channel estimation, where the existence of impulsive noise is explicitly considered during channel estimation. Interestingly, it can be seen from Table II that as the T83 file is only slightly affected by impulsive noise, an improved channel estimation together with channel coding are sufficient to obtain a zero coded BER over the investigated data.

The INC step of the proposed algorithm can further improve the system performance by around 2-3% in raw BER (both T84 and T85), 6% in coded BER (T84, 1/3 rate), and 9% in coded BER (T84 and T85, 1/2 rate), compared with the proposed algorithm without the INC. It can also been seen from Tables II-IV that the proposed algorithm with INC outperforms the LS estimator with the blanking operation and significantly reduces the system FER.

V. CONCLUSIONS

We have proposed a novel CS based joint channel estimation and impulsive noise cancelation algorithms for UA OFDM systems. The proposed algorithm is applied to process the data collected during a UA communication experiment. The results show that the proposed approach significantly improves the performance of both channel estimation and impulsive noise cancelation of UA OFDM systems.

REFERENCES

[1] D. Kilfoyle and A. Baggeroer, "The state of the art in underwater acoustic telemetry," *IEEE J. Oceanic Engineering*, vol. 25, no. 1, pp. 4–27, Jan. 2000.
[2] M. Stojanovic and L. Freitag, "Multichannel detection for wideband underwater acoustic CDMA communications," *IEEE J. Oceanic Engineering*, vol. 31, no. 3, pp. 685–695, July 2006.
[3] B. Li, S. Zhou, M. Stojanovic, L. L. Freitag, and P. Willett, "Multicarrier communication over underwater acoustic channels with nonuniform Doppler shifts," *IEEE J. Oceanic Engineering*, vol. 33, no. 2, pp. 198–209, 2008.
[4] H. Yan, L. Wan, S. Zhou, Z. Shi, J. H. Cui, J. Huang, and H. Zhou, "DSP based receiver implementation for OFDM acoustic modems," *Physical Communication*, vol. 5, no. 1, pp. 22–32, Mar. 2012.
[5] M. Chitre, S. H. Ong, and J. Potter, "Performance of coded OFDM in very shallow water channels and snapping shrimp noise," in *Proc. MTS/IEEE OCEANS*, Washington, DC, Sep. 2005, pp. 996–1001.
[6] H. Sun, W. Shen, Z. Wang, S. Zhou, X. Xu, and Y. Chen, "Joint carrier frequency offset and impulse noise estimation for underwater acoustic OFDM with null subcarriers," in *Proc. MTS/IEEE OCEANS*, Hampton Roads, VA, Oct. 2012.
[7] J. A. Tropp and A. C. Gilbert, "Signal recovery from random measurements via orthogonal matching pursuit," *IEEE Trans. Inf. Theory*, vol. 53, pp. 4655-4666, Dec. 2007.